Cerebral Cortex May 2013;23:1218–1229
doi:10.1093/cercor/bhs115
Advance Access publication May 3, 2012

Plasminogen Activator Inhibitor-1 Mitigates Brain Injury in a Rat Model of Infection-Sensitized Neonatal Hypoxia–Ischemia

Dianer Yang[1], Yu-Yo Sun[1], Niza Nemkul[1], Jessica M. Baumann[1], Ahmed Shereen[2], R. Scott Dunn[2], Marsha Wills-Karp[3], Daniel A. Lawrence[5], Diana M. Lindquist[2] and Chia-Yi Kuan[1,4]

[1]Division of Developmental Biology, [2]Department of Radiology, Imaging Research Center, [3]Division of Immunobiology, and [4]Division of Neurology, Cincinnati Children's Hospital Medical Center, Cincinnati, OH 45229, USA [5]Deptartment of Internal Medicine, Division of Cardiovascular Medicine, University of Michigan Medical School, Ann Arbor, MI 48109, USA

Address correspondence to Chia-Yi Kuan. Email: alex.kuan@cchmc.org.

Intrauterine infection exacerbates neonatal hypoxic–ischemic (HI) brain injury and impairs the development of cerebral cortex. Here we used low-dose lipopolysaccharide (LPS) pre-exposure followed by unilateral cerebral HI insult in 7-day-old rats to study the pathogenic mechanisms. We found that LPS pre-exposure blocked the HI-induced proteolytic activity of tissue-type plasminogen activator (tPA), but significantly enhanced NF-κB signaling, microglia activation, and the production of pro-inflammatory cytokines in newborn brains. Remarkably, these pathogenic responses were all blocked by intracerebroventricular injection of a stable-mutant form of plasminogen activator protein-1 called CPAI. Similarly, LPS pre-exposure amplified, while CPAI therapy mitigated HI-induced blood-brain-barrier damage and the brain tissue loss with a therapeutic window at 4 h after the LPS/HI insult. The CPAI also blocks microglia activation following a brain injection of LPS, which requires the contribution by tPA, but not the urinary-type plasminogen activator (uPA), as shown by experiments in *tPA*-null and *uPA*-null mice. These results implicate the nonproteolytic tPA activity in LPS/HI-induced brain damage and microglia activation. Finally, the CPAI treatment protects near-normal motor and white matter development despite neonatal LPS/HI insult. Together, because CPAI blocks both proteolytic and nonproteolytic tPA neurotoxicity, it is a promising therapeutics of neonatal HI injury either with or without infection.

Keywords: diffusion tensor imaging (DTI), neonatal hypoxia–ischemia, plasminogen activator inhibitor-1 (PAI-1), tissue plasminogen activator (tPA), white matter injury

Introduction

Perinatal hypoxic–ischemic (HI) insult is a major threat to the development of cerebral cortex (Volpe 2003; Khwaja and Volpe 2008). Moreover, perinatal infection amplifies the HI brain injury, often resulting in neonatal mortality or permanent neurological deficits, such as cerebral palsy, epilepsy, white matter (WM) reduction, and cognition impairment (Perlman 1998; Adams-Chapman and Stoll 2006; Allin et al. 2011). Hence, the development of effective therapies of infection-sensitized HI brain injury is an important issue in modern neonatal care.

Studies in animal models suggested that prenatal infection (chorioamnionitis) and the ensuing fetal inflammatory response amplify brain damage via innate immunity and microglia activation (Lehnardt et al. 2003; Eklind et al. 2005). These discoveries, however, have not led to effective therapies, because systemic immune suppression in infants will increase the risk of severe infection, which already accounts for up to 25% of neonatal death (Lawn et al. 2005). Thus, targeted inhibition of the brain microglia activation is a safer and perhaps more effective therapy for neonatal infection/HI injury (Ransohoff and Perry 2009).

Tissue-type plasminogen activator (tPA) is a potential target to suppress microglia activation in the newborn brain. tPA has multiple functional domains, including a C-terminal protease domain, 2 kringle domains that interact with the *N*-methyl-D-aspartate receptor subunit, an epidermal growth factor-like domain, and an N-terminal finger domain that mediates microglia activation independent of the protease domain (Rogove et al. 1999; Siao and Tsirka 2002; Zhang et al. 2007, 2009; Yepes et al. 2009). We recently reported that anti-tPA treatment with a stable-mutant form of plasminogen activator inhibitor-1 (PAI-1) called CPAI markedly reduced HI-triggered tPA proteolytic activity and destruction of newborn brains (Berkenpas et al. 1995; Adhami et al. 2008; Yang et al. 2009). These findings suggest that hyper-stimulation of the parenchymal tPA activity is an important mechanism of neonatal HI brain injury, but whether CPAI protects against infection-sensitized HI injury is unknown.

Another unanswered question is whether infection merely upregulates the severity of neonatal HI insult or fundamentally changes the nature of brain response to HI. The notion of an infection-altering response to HI warrants consideration, because in pure-HI brain injury microglia are activated secondary to tissue damage in a "sterile inflammation" manner (Chen and Nunez 2010), but they are pre-activated by prenatal infection and may thereby create a different milieu for the subsequent HI response. Consistent with this notion, while the mouse pups lacking myeloid differentiation primary response gene 88 (MyD88)—a critical downstream mediator of innate immunity—had high resistance to lipopolysaccharide (LPS)-sensitized HI insults, they were equally sensitive to pure-HI insult like wild-type animals (Wang et al. 2007). The intriguing differential responses raised the possibility that pure- and infection-sensitized HI may trigger divergent pathogenic mechanisms in immature brains. Key switch of the differential responses, however, is yet to be determined.

To investigate these issues, we compared the response with pure-HI and dual LPS/HI insults and the therapeutic effect of CPAI in neonatal rat brains. Our results indicated that LPS pre-exposure significantly decreased the HI-induced tPA proteolytic activity but amplified the NF-κB signaling pathway, thus in effect altering the brain response to HI. Interestingly, CPAI therapy not only reduced HI insults, but also mitigated microglia activation and LPS/HI-induced neuroinflammation and brain injury. Together, these results suggest that CPAI is a promising therapeutics of pure- and infection-sensitized HI injury in newborns.

Materials and Methods

Animal Surgery

The experimental model of LPS-sensitized neonatal hypoxia was performed as previously described (Eklind et al. 2005; Yang et al. 2009). Briefly, 0.3-mg/kg LPS was injected intraperitoneally to 7-day-old Wistar rat pups at 4 h before the induction of unilateral cerebral HI with the Rice-Vannucci model. This low-dose LPS was used to mimic subclinical infection as previously described (Lehnardt et al. 2003; Eklind et al. 2005; Wang et al. 2007), and no apparent impairment of animals was observed. The pups were anesthetized by 3% isoflurane mixed with pure oxygen while the right common carotid artery was ligated. After a 1-h recovery period, pups were placed in glass chambers containing a humidified atmosphere of 10% oxygen and 90% nitrogen and submerged in a 37°C water bath. After an 80-min hypoxia period—a relatively short duration of hypoxia that does not produce severe brain injury in animals without LPS pretreatment (see Fig. 1)—intracerebroventricular (ICV) injection of 10 μL saline or 1.9 μg CPAI (a stable-mutant form of human PAI-1 with 4 amino acid substitutions, N150H, K154T, Q319L, and M354I, Molecular Innovations Inc., Novi, MI, USA) was performed with a Hamilton syringe at 10 min, 2 h, or 4 h post-hypoxia, using the following coordinates as previously described: 2.0 mm rostral and 1.5 mm lateral to the right from the Lamda point and at a depth of 2.0 mm from the surface of the brain (Yang et al. 2009). The generation of *tPA*- and urinary-type plasminogen activator (*uPA*)-null mice has been reported, and these mice have been crossed to the C57BL/6 strain for >10 generations (Carmeliet et al. 1994). The surgical procedures were approved by the Institutional Animal Care and Use Committee and conformed to the NIH Guidelines for Care and Use of Laboratory Animals.

Diffusion Tensor Imaging

Ex vivo diffusion tensor imaging (DTI) on fixed brains was performed as previously described (Shereen et al. 2011). Due to the lower signal-to-noise ratio and lower resolution of in vivo DTI in small rodent brains, ex vivo imaging was performed to assess the damage in the WM structures. All data were acquired on a Bruker BioSpec 7T system with 40 G/cm gradients using a custom-built solenoid transmit–receive coil. Whole brain data were collected using a three-dimensional, conventional spin-echo DTI sequence with the following parameters: $b = 800$ s/mm^2 gradient separation/duration ($\Delta/\delta = 12/4$ ms, 6 diffusion gradient directions and 1 b_0 image, field-of-view = $32 \times 12 \times 12$ mm^3, matrix = $256 \times 96 \times 96$, resolution = 125 μm isotropic, echo time = 24 ms, and repetition time=1 s). The total scan time was approximately 18 h. Quantification of DTI measures including fractional anisotropy (FA), axial diffusivity (λ_{II}), and radial diffusivity ($\lambda_{\perp}$) was performed using the DTIstudio software.

Assessment of Brain Damage

Brain damage was measured by the extent of tissue loss at 7 days after infection-sensitized neonatal hypoxia–ischemia insults as previously described (Adhami et al. 2008; Yang et al. 2009). Briefly, pups were sacrificed under deep anesthesia by transcardiac perfusion of saline and then 4% paraformaldehyde. Following post-fixation, the brains went through sucrose gradients and were frozen in tissue-freezing medium, then cut into coronal sections at 50-μm thickness. Eight evenly spaced sections were taken to represent the whole brain and stained by 2% cresyl violet. Every section was photographed and analyzed using the NIH Image J software to quantify the surface area of cerebral cortex, striatum, and hippocampus on the lesion and contralateral sides. The percentage of tissue loss was calculated at every relevant section for each structure as a ratio of lesion to contralateral areas, and this was averaged over 8 sections for each animal.

Assessment of Blood-Brain-Brain Permeability

The blood-brain-brain (BBB) barrier permeability was determined as previously described (Lenzser et al. 2007). Briefly, 5% sodium fluorescein (NaF) (Sigma-Aldrich, St. Louis, MO, USA) solution was injected intraperitoneally to rat pups at the dosage of 10 μL/g of body weight. Two hours later, animals were sacrificed by transcardial perfusion of saline to wash out NaF in the blood stream. The brains were removed and photographed using a fluorescence stereomicroscope. The cerebral cortex was then cut into halves and each hemisphere was homogenized with 500 μL trichloroacetic acid (80%) and centrifuged for 10 min at $13\,600 \times g$. An aliquot of 150-μL supernatant added with 50 μL of 5 M NaOH were mixed in triplicates in a 96-well microplate and measured by a spectrophotometer with the absorption wave length at 490 nm.

Plasminogen Activator Zymogram

The plasminogen activator zymography was performed as previously described (Adhami et al. 2008; Yang et al. 2009). Briefly, plasminogen and casein were added to the sodium dodecyl sulfate–polyacrylamide gel electrophoresis (SDS–PAGE) gel. Protein samples were extracted using the radioimmunoprecipitation assay and mixed with 2× sample buffer (0.5 M Tris–HCl, pH 6.8, 100% glycerol, 0.05% bromophenol blue, 10% SDS) without boiling before electrophoresis carried out using a low voltage for up to 5 h. Recombinant human tPA (Activase, Genetech, San Francisco, CA, USA) was used as positive controls. After electrophoresis, the gel was rinsed twice in 2.5% Triton-X-100 at room temperature for 30 min each, followed by incubation in glycine buffer (0.1 M glycine, pH 8.0) at 37°C overnight. The gel was stained by Coomassie blue solution and destained to reveal the lytic zones of protease activity. The zymogram gel was photographed and presented in a black-and-white inverted image. Quantification was performed using the NIH Image J software to determine the size of the lytic zones.

Matrix Metalloproteinase Zymogram

The matrix metalloproteinase (MMP) zymography was performed as previously described (Adhami et al. 2008; Yang et al. 2009). Briefly, 0.15% porcine skin gelatin was added to the SDS–PAGE gel. Protein samples were extracted and run in the same condition as for plasminogen activator zymogram. After electrophoresis, gels were washed twice with 2.5% Triton-X-100, incubated in reaction buffer (50 mM Tris, pH 7.5, 200 mM NaCl, 5 mM $CaCl_2$) at 37°C overnight, then stained and de-stained with Coomassie blue solution.

In vitro tPA Activity Assay

In vitro tPA activity was measured using the Chromolize™ tPA assay kit (Catalog No. 1103, Trinity Biotech, Inc., Wicklow, Ireland) following the manufacturer's instructions. Briefly, 100 μL of tPA standards (0, 0.5, 1.0, 1.5, and 2.0 IU/mL) and samples were added to a 96-well plate. After mixing and washing for 20 min, 50 μL substrate reagent was added to each well using the repeating pipette, followed by the addition of 50 μL plasminogen reagent. The reaction was carried out at ambient temperature with gentle shaking for 90 min. The reaction activity was measured using a 96-well spectrophotometer with the absorbance at 405 nm.

Cytokine Array and Enzyme-linked Immunosorbent Assay

Cytokine array was performed as previously described using the ChemiArray antibody array system (Millipore, Billerica, MA, USA) and following the manufacturer's instructions (Yin et al. 2007). Rat MCP-1 was measured using a commercial Enzyme-linked Immunosorbent Assay (ELISA) kit (# R0608001C, RayBiotech, Norcross, GA, USA). Mouse MCP-1 was measured using specific antibodies (# 506002, Biolegend, San Diego, CA, USA). Rat and mouse tumor necrosis factor-alpha (TNFα) was measured using a cross-species-reactive antibody (AF-410-NA, R&D Systems, Minneapolis, MN, USA).

NF-κB Electrophoresis Mobility Shift Assay

NF-κB electrophoresis mobility shift assay (EMSA) was carried out using the Lightshift Chemiluminescent kit (Catalog No. 20148, Thermo Fisher Scientific, Waltham, MA, USA). Briefly, 5 μL nuclear extract from brains, 2 μL binding buffer, 1 μL poly-dIdC, 1 μL biotin-

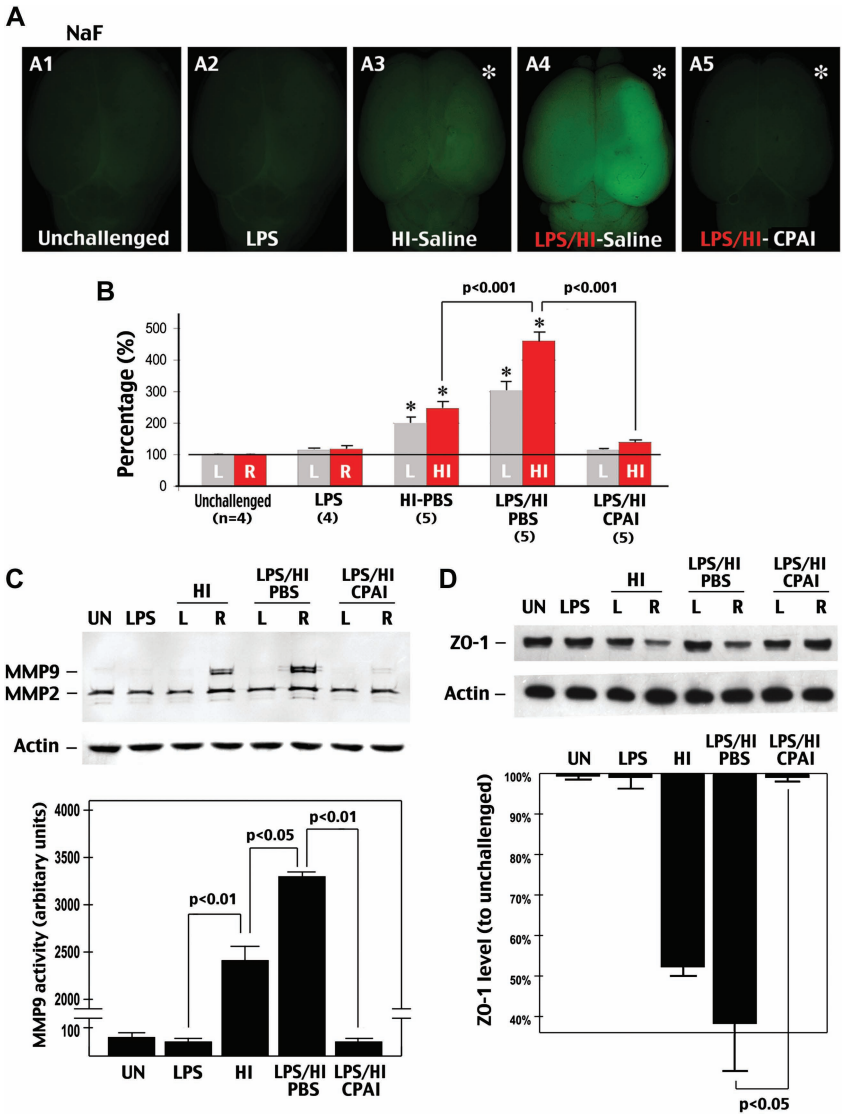

Figure 1. CPAI prevents LPS/HI-induced BBB damage in immature brains. (*A*) Representative photographs of the brains from P8 rat pups treated with the indicated conditions (A1–A5) 24 h earlier and injected intraperitoenally with NaF at 2 h prior to sacrifice and transcardial perfusion ($n = 4$–5 as indicated in *B*). (*B*) Quantification of the NaF fluorescence from brain extracts. LPS/HI insults increased the extravascular NaF fluorescence to 461 ± 26% (mean ± SEM) of the baseline level in the carotid-occluded hemisphere (HI, asterisk in *A*). L, the opposite (left) side of brain; R, the right side of brain. $^*P < 0.01$ by unpaired *t*-test. (*C*) Representative MMP zymogram at 24 h after the indicated treatment conditions ($n = 4$). Equal loading of brain extracts was verified by the immunoblot detection of β-actin. The optic density of MMP-9 bands was quantified (lower panel). The *P*-value was determined using unpaired *t*-test. (*D*) Representative immunoblotting against ZO-1 at 24 h after the indicated treatments ($n = 3$). Quantification (lower panel) showed that LPS/HI insults reduced the ZO-1 level to 36 ± 13% (mean ± SEM) of the baseline level, while CPAI treatment prevented the decrease of ZO-1 (98 ± 2%). $P < 0.05$ by unpaired *t*-test. Note that LPS administration by itself had little effects, but its addition to HI amplified NaF extravasation, MMP-9 activation, and ZO-1 reduction, which were all markedly mitigated by post-LPS/HI administration of CPAI.

labeled oligonucleotide probe and 1 μL super-pure water were mixed and spin down to the bottom of the tube and incubated at room temperature for 30 min. The sample was then loaded to nondenaturing 5% polyacrylamide gel and run for 2.5 h in 0.5× Tris/Borate/EDTA buffer. The binding reactions were electrophoretically transferred to nylon membrane under 300 mA for 45 min and UV cross-linked. The positions of biotin-labeled probe were detected using streptavidin-conjugated chemiliminescence and X-ray film. The sequences of oligonucleotide probes containing normal or mutant NF-κB enhancer-binding sites were identical to those previously described (Zhang et al. 2007; Nijboer et al. 2008).

Immunoblot Analysis

Brain samples for immunoblots were homogenized in 1× TLB (1% Triton X-100, 20 mM Tris, pH 7.4, 137 mM NaCl, 25 mM β-glycerophosphate, 25 mM Na-pyrophosphate, 2 mM EDTA, 1 mM Na_3VO_4, 10% glycerol, 1 mM phenylmethylsulfonyl fluoride, 0.7% protease inhibitor cocktail). The proteins were separated by standard SDS–PAGE procedures, electro-transferred onto a polyvinylidene fluoride microporous membrane (Bio-Rad, Hercules, CA, USA) and detected with designated antibodies followed by the enhanced chemilluminescence detection (Amersham Biosciences). The antibodies used are: anti-ZO1 (Zymed), anti-PAI-1 (Molecular Innovations), anti-IκBα (Cell Signaling Technology), and anti-β-actin (Sigma).

Behavioral Testing

Rats were placed on the elevated accelerating rotating rod (3 cm in diameter) beginning at 4 rpm/min for 4 trials per day, during which time the rotating rod underwent acceleration from 4 to 40 rpm over 3 min and then remained at the maximum speed for another 3 min. Animals were scored for their latency (in microseconds) to fall in each

trial. Animals rested a minimum of 10 min between the trials to avoid fatigue.

Histology

All immunohistochemistry was performed on 20-μm-thick frozen sections using standard procedures. The following antibodies were used: a rabbit anti-Iba1 (Wako) and a mouse anti-CD11b/c (OX42) (DAKO) antibody. Secondary antibody was conjugated to Alexa Fluor488 or Alexa Fluor 94 (Molecular Probes).

Statistical Analysis

Values are represented as mean ± SD or SEM as indicated. Quantitative data were compared between different groups using one-way ANOVA or 2-sample (unpaired) *t*-test assuming an equal variance.

Results

LPS Pre-Exposure Increases HI-Induced BBB Damage and MMP-9 Activation, and CPAI Treatment Protects Against Combined LPS/HI Insults

To simulate subclinical infection, we injected a single, low-dose LPS (0.3 mg/kg) to P7 rat pups intraperitoneally at 3 h before unilateral ligation of the common carotid artery, and thus 4 h before the induction of 80 min hypoxia (10% oxygen). This relatively short duration of hypoxia was chosen to test whether LPS pre-exposure sensitizes HI brain injury. In initial experiment, we measured the brain permeability to NaF and the MMP-9 activity at 24 h recovery as the indication of BBB damage. This experiment showed that LPS injection alone had very little effect on the BBB permeability to NaF, but when combined with a mild HI insult, it markedly increased NaF extravasation in the carotid-ligated hemisphere (Fig. 1*A* and *B*; $n = 4$–5 for each group). Similarly, although IP injection of LPS produced no obvious MMP-9 activity, dual LPS/HI insult induced higher MMP-9 activity (Fig. 1*C*, $P < 0.05$; $n = 4$ for each group) and NaF extravasation than HI alone (Fig. 1*B*, $P < 0.001$). In addition, either LPS/HI or pure-HI insult, but not LPS injection per se, reduced the amount of a tight-junction protein ZO-1 in the newborn rodent brain (Fig. 1*D*, $n = 3$). Of note, HI and LPS/Hi insults caused mild NaF extravasation on the contralateral hemisphere where no MMP-9 activation or histological damage was detected. The discrepancy is likely because NaF (376 Da) permeates BBB through a paracellular pathway, which does not require extensive MMP activation (Hawkins and Egleton 2008).

Interestingly, intracerebroventricular injection of 1.9 μg CPAI—a dose that reduced pure-HI insults in rat pups (Yang et al. 2009)—almost completely prevented LPS/HI-induced NaF extravasation (Fig. 1*A*(A5), *B*, $P < 0.01$ by *t*-test;), MMP-9 activation (Fig. 1*C*, $P < 0.01$), and ZO-1 reduction (Fig. 1*D*, $P < 0.05$ compared with saline-treated animals; CPAI was injected at 10 min post-hypoxia in all experiments unless mentioned otherwise). These data suggest that while exposure to low-dose LPS per se causes no apparent injury in immature brains, its addition to HI greatly magnifies BBB damage, but therapeutic administration of CPAI may protect against LPS-sensitized neonatal HI injury.

LPS/HI Induces NF-κB Signaling at the Expense of Proteolytic tPA Activity, but Is Inhibited by the CPAI Therapy

To investigate the mechanism of infection/LPS-sensitized HI injury and CPAI-mediated protection, we first examined the distribution and clearance of ICV-injected CPAI (Fig. 2*A*; arrow indicates the injected right hemisphere, R). Immunoblot analysis with an anti-human/rat PAI-1 antibody showed no detectable PAI-1 expression in the brain of unchallenged animals. The exogenous CPAI was evenly distributed in both hemispheres at 1 h after ICV injection and almost completely disappeared in the brain by 2 h (Fig. 2*A*).

Next, we tested whether LPS magnifies nonvascular tPA activity to impose greater tissue proteolysis in newborn brains. Surprisingly, biochemical analysis showed that, while LPS exposure by itself had little effect, its addition to a secondary HI insult significantly reduced tPA activity on the HI-stressed hemisphere at 4 h post-hypoxia without changing its protein level, similar to the effect of ICV–CPAI injection (Fig. 2*B*, the right, R, hemisphere is the carotid-ligated side in all displays throughout the article). Quantification showed that LPS/HI and CPAI-injection reduces the tPA proteolytic activity to 54.7% and 59% of the basal level, respectively, while even brief 80-min HI challenge increases the tPA activity to 134%; $n = 5$). At 24 h recovery, the LPS/HI-challenged hemisphere showed a normal level of tPA proteolytic activity, an increased uPA activity—a general indicator of neural stress or brain injury—similar to those subjected to pure-HI insult (Fig. 2*E*, 376% and 404%, respectively, $n = 5$), and expression of the endogenous PAI-1 that was absent in either LPS or pure-HI challenge or the contralateral hemisphere of LPS/HI-injured brains (Fig. 2*C*). Interestingly, immunoblotting analysis showed that the ICV-injected CPAI had a delayed clearance in the carotid-ligated hemisphere up to 4 h (R in Fig. 2*B*), which could inhibit the tPA proteolytic activity by forming a tighter tPA–CPAI complex than endogenous PAI-1 that was induced at 24 h recovery. The mechanism of tPA inhibition in the acute phase following LPS/HI insult remains unclear and warrants future investigation.

Next, because it has been reported that IP injection of LPS triggers innate immune responses in newborn brains, we examined the effects of LPS/HI and CPAI injection on the downstream NF-κB signaling pathway (Lehnardt et al. 2003; Wang et al. 2009). Biochemical analysis showed that dual LPS/HI insult diminished the amount of cytoplasmic IκBα (Fig. 2*F*) and markedly increased the nuclear NF-κB DNA-binding activity at 4 h post-hypoxia (Fig. 2*G*). Remarkably, ICV injection of CPAI after LPS/HI almost completely prevented IκBα \xEF\x80depletion (Fig. 2*F*, $n = 3$) and nuclear NF-κB activity in neonatal brains (Fig. 2*G*, $n > 6$ sets).

These results suggest that LPS pre-exposure changes the pathogenic response to HI in neonatal brains, rendering a shift from tPA proteolysis to escalation of NF-κB signaling in the acute phase to produce greater tissue destruction.

CPAI Attenuates LPS/HI-Induced Monocyte Chemoattractant Protein-1 Synthesis and Monocyte Entry in the Newborn Brain

The NF-κB signaling pathway regulates the synthesis of pro-inflammatory cytokines (Nijiboer et al. 2008). To test

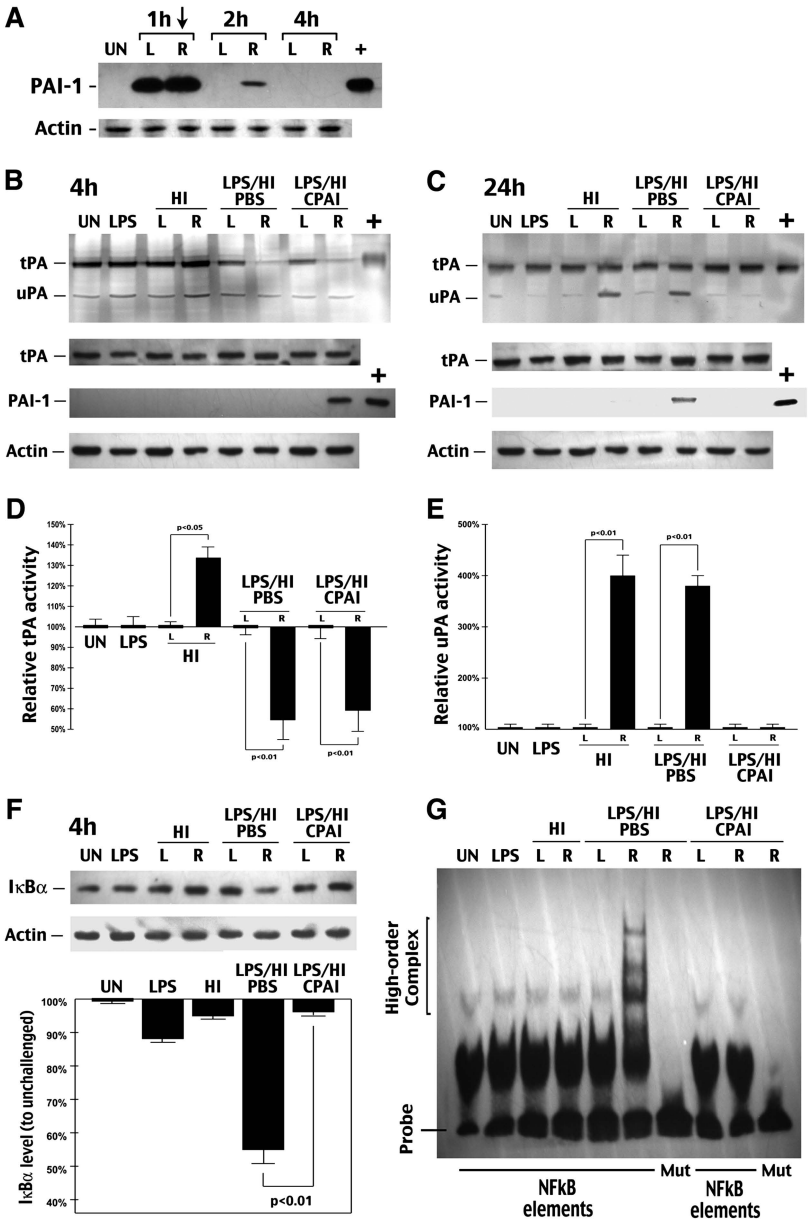

Figure 2. CPAI prevents LPS/HI-induced NF-κB signaling activation in immature brains. (*A*) Immunoblot analysis of the distribution and clearance of CPAI injected unilaterally to the lateral ventricle (arrow) in P7 rat pups. R, right hemisphere; L, left hemisphere. Note the undetectable basal level of PAI-1 in the brain parenchyma, diffusion of injected CPAI in both hemispheres, and a rapid decline of the CPAI level at 2 h post-intracerebrventricular (ICV) injection. (*B* and *C*) Representative photographs of plasminogen–zymogram and immunoblot-detection of tPA, PAI-1, or β-actin from brain extracts of rat pups at 4 (*B*) or (*C*) 24 h after the indicated conditions ($n = 5$). +, positive-control lanes were loaded with recombinant tPA or CPAI. The optic density of tPA band at 4 h and uPA band at 24 h was quantified for each condition for comparison (lower panel). Note the strong inhibition of tPA activity at 4 h in saline- or CPAI-treated brains following LPS/HI insult, as well as the induction of uPA activity at 24 h in both HI- and LPS/HI-challenged brains without the CPAI treatment. (*F*) Immunoblot detection of IκBα from whole-cell lysates of the brains collected at 4 h after the indicated conditions ($n = 3$). L, the opposite/left hemisphere. R, the carotid-occluded (right) hemisphere. Quantification after normalized to β-actin (lower panel) showed that LPS/HI decreased IκBα to 55 ± 4% (mean ± SEM) of the basal level in unchallenged brains, while post-HI administration of CPAI almost completely prevented IκBα reduction (96 ± 1% of the baseline); $P < 0.01$ by unpaired *t*-test. (*G*) Representative NF-κB EMSA gel using the nuclear extract of brains collected at 4 h after indicated conditions ($n > 6$). Mut, oligonucleotide probes with mutated NF-κB binding sequence. Note that the high-order protein–DNA complex was detected only in the sample from LPS/HI-injured brains, which was abolished by the CPAI treatment.

whether the induction of NF-κB activity and its suppression by CPAI in the acute phase of LPS/HI insult translates into changes in the brain cytokine level at 24 h recovery, we performed a multiplex antibody array and found that LPS/HI significantly increased the brain monocyte chemoattractant protein-1 (MCP-1) to 9.75-fold of the baseline level ($n = 4$), which was reduced to 3.13-fold by CPAI ($n = 4$) (Fig. 3*A*). Further analysis by ELISA confirmed a greater increase in the brain MCP-1 level at 24 h after LPS/HI insult than pure-HI, as well as a significant attenuation by the CPAI treatment (Fig. 3*B*, $n = 4$, $P < 0.05$ by *t*-test). In contrast, LPS, pure-HI, and dual LPS/HI challenge all elevated the blood MCP-1 level to a similar degree, which was not diminished by the CPAI treatment (Fig. 3*C*).

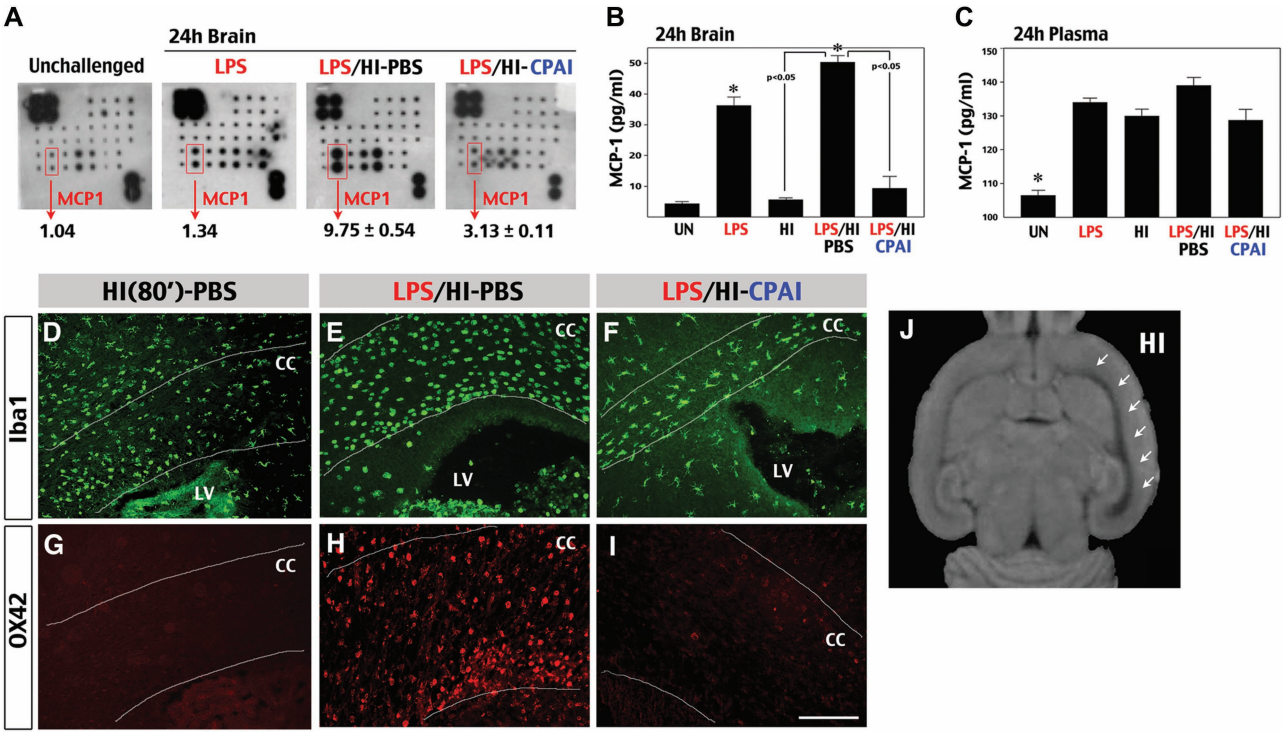

Figure 3. CPAI prevents LPS/HI-induced chemokine production and monocyte recruitment. (*A*) Representative results of a cytokine array using brain extracts at 24 h following indicated conditions ($n = 2$ for unchallenged and LPS-treated animals; $n = 4$ for LPS/HI-PBS or LPS/HI-CPAI treatments). The duplicated spots of MCP-1 and the quantification results were indicated. LPS/HI increased the brain MCP-1 level to 9.75 ± 0.54 (mean ± SD) fold of the baseline level, while CPAI treatment attenuated this induction. (*B* and *C*) ELISA analysis of the MCP-1 levels from brains (*B*) or the plasma (*C*) at 24 h after the indicated conditions ($n = 4$ for each). The MCP-1 level in the unchallenged brain was 4.4 ± 0.85 pg/mL extracts (mean ± SD), which was increased by LPS/HI insults to 50.3 ± 4.4 pg/mL (asterisk, $P < 0.01$) and significantly attenuated by the CPAI treatment ($P < 0.05$ by unpaired *t*-test). In contrast, the basal plasma MCP-1 level was already high in unchallenged animals (116.7 ± 3.3 pg/mL), and upregulated by various stimuli to a similar degree. (*D–I*) Immunofluoresence detection of Iba1 (*D*, *E*, and *F*) and OX42/CD11b (*G*, *H*, and *I*) in coronal sections at the fornix-decussation level of brains collected at 16 h after pure-HI, LPS/HI-PBS, or LPS/HI-CPAI treatments ($n > 5$). White lines mark the boundaries of corpus callosum (CC). LV, lateral ventricles. Scale bar: 50 μm. Note that the CC in LPS/HI-PBS-treated rats was 2 times wider than that of LPS/HI-CPAI-treated rats and filled with numerous large, round Iba1/OX42 double-positive cells (248 ± 24 per visual field). In contrast, LPS/HI-CPAI-treated animals contained fewer Iba1+ cells within the corpus callosum (50 ± 11 per visual field) that exhibited ramified cytoplasmic processes and did not express OX42. Also note that the swelling of CC was milder in pure-HI-injured animal brains and there was no obvious OX42-immunoreactivity. (*J*) The tensor trace map from rat brain at 24 h after LPS/HI insult. Note the expansion/swelling of CC/external capsule on the HI-injured hemisphere (indicated by arrows).

The inability to suppress the blood MCP-1 level by CPAI injection may attribute to a high baseline value in unchallenged animals. Alternatively, brain-specific reduction of MCP-1 by the CPAI treatment may be sufficient to prevent LPS/HI-induced microglia activation and the infiltration of immune-response cells (Ivacko et al. 1997; Galasso et al. 2000; Deng et al. 2009). To test this possibility, we examined the morphology and distribution of Iba1+ and OX42/CD11b+ microglia/monocytes at 16 h recovery in the brains of pure-HI (80 min)-challenged pups and those receiving post-LPS/HI injection of saline or CPAI (Fig. 3*D–I*). This analysis showed a swollen corpus callosum filled with Iba1/OX42 double-positive cells in the LPS/HI-injured pups receiving saline-injection (Fig. 3*E* and *F*), but not in pure-HI injured (Fig. 3*D*, D) or LPS/HI-challenged but CPAI-treated animals (Fig. 3*F* and *I*). The enlargement of WM in LPS/HI-injured pups was also detected by the tensor trace magnetic resonance imaging (arrows in Fig. 3*J*). Moreover, while Iba1+ microglia in pure-HI-challenged or CPAI-treated pups showed ramified processes (Fig. 3*D* and *F*), their counterparts in LPS/HI-injured and saline-treated pups showed a large, rounded morphology and strong OX42-immunoreactivity (Fig. 3*D* and *F*), which is typical for phagocytic microglia or monocytes/macrophages (Ransohoff and Perry 2009). Together, these results suggest the CPAI therapy mitigates LPS/HI-induced microglia activation and MCP-1 expression, leading to decreased monocyte infiltration as part of the neuroprotection mechanism.

CPAI Inhibits LPS-Induced and tPA-Dependent Microglia Activation

Growing evidence suggests that microglia have a critical role in infection-sensitized neonatal HI brain injury (Khwaja and Volpe 2008). Because tPA directly interacts with the cell surface receptors on microglia to activate them, and since CPAI sequesters tPA in a tight complex, it seems likely that CPAI may have a direct inhibitory effect on microglia activation (Berkenpas et al. 1995; Siao and Tsirka 2002). To test this possibility, we used an established paradigm of microglia activation by ICV injection of LPS in P7 rat pups (Lund et al. 2006) and infused PBS or 1.9 μg CPAI into the lateral ventricle in the opposite hemisphere ($n = 4$ for each). The brains were harvested 24 h later to measure TNFα and MCP-1 levels by ELISA. This analysis showed that CPAI prevented TNFα induction and significantly diminished LPS-induced MCP-1 expression (Fig. 4*A* and *B*, $P < 0.01$ by *t*-test).

Because CPAI inhibits both tPA and the uPA, we wish to determine which plasminogen activator is more important for infection/LPS-induced microglia activation. To address this

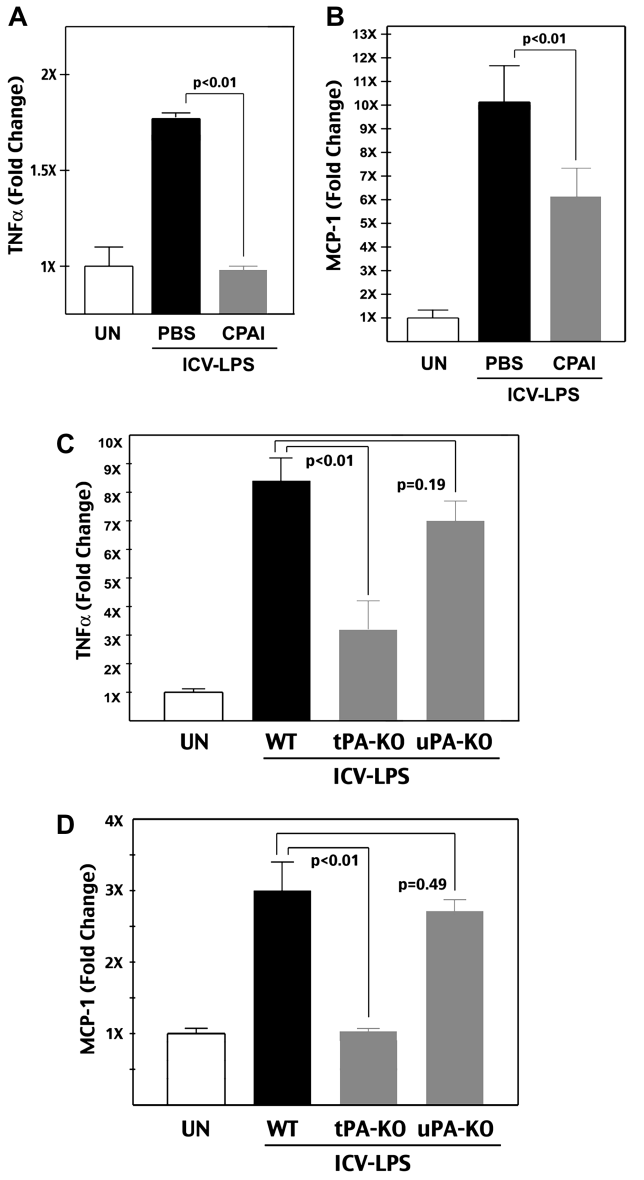

Figure 4. CPAI mitigates LPS-induced and tPA-dependent cytokine production. (*A* and *B*) ELISA measurement of the TNFα and MCP-1 level in the brains of P8 rats at 24 h after intracerebroventricular injection of 1.9 μg LPS, as well as saline (PBS) or 1.9 μg CPAI injection on the opposite cerebral ventricle, normalized to unchallenged (UN) animals ($n = 4$ for each group). Note that ICV injection of LPS increased both TNFα (172 ± 2%; mean ± SD) and MCP-1 (1026 ± 150%) levels in the brain, which were significantly attenuated by CPAI treatment (96 ± 2% for TNFα and 612 ± 145% for MCP-1, $P < 0.01$ by unpaired *t*-test). (*C* and *D*) ELISA measurement of the TNFα and MCP-1 level in the brains of P10 wild-type, *tPA*-null, and *uPA*-null mice at 24 h after ICV injection of 20 μg LPS ($n = 5$ for unchallenged and LPS injection groups of each genotype). An LPS injection increased both TNFα (834 ± 88%; mean ± SE) and MCP-1 levels (297 ± 36%) in wild-type mice, but only mildly affected the expression of TNFα (336 ± 78%) and MCP-1 (104 ± 2%) in *tPA*-null mice. The increase of TNFα (724 ± 51%) and MCP-1 (269 ± 15%) levels in *uPA*-null mice was not significantly different from that in wild-type mice.

issue, we applied ICV–LPS injection in P10 *tPA*-null, *uPA*-null, or wild-type mouse pups and compared the brain levels of TNFα and MCP-1 24 h later ($n = 5$ for each group). This analysis showed that only tPA, but not uPA, deficiency significantly attenuated LPS-induced cytokine production (Fig. 4*C* and *D*, $P < 0.01$ by *t*-test). These results support the notion of tPA predominance over uPA in microglia activation (Tsirka et al. 1997). Yet, because *tPA*-null mice have a very high mortality rate in acute HI insult due to thrombosis (Adhami et al. 2008), they cannot be used to test the requirement of tPA for LPS/HI-induced neuroinflammatory responses directly.

CPAI Decreases LPS/HI-Induced Brain Damage with an Effective Window at 4 h After Insult

Next, we examined the effect of CPAI treatment in preserving brain tissue following LPS/HI insults. In this experiment, a single-dose 1.9 μg CPAI or PBS was ICV injected into P7 rat pups at 10 min, 2 h, or 4 h after hypoxia ($n = 17$–20 for each group as indicated in Fig. 5*C*). The brains of challenged animals were collected at P14, photographed (Fig. 5*A* and *B*), serially sectioned, and Nissl stained to quantify the tissue loss in the cerebral cortex, hippocampus, and striatum compared with counterparts on the contralateral hemisphere.

This analysis showed that the majority of PBS-injected pups developed severe brain atrophy in the carotid-ligated hemisphere (arrows in Fig. 5*A*), while those receiving acute CPAI treatment were mostly free of destruction (Fig. 5*B*). Quantification showed that, in PBS-injected animals ($n = 19$), there was 43 ± 2.5% tissue loss (mean ± SEM) in the cerebral cortex, 44.2 ± 3.9% in the hippocampus, and 29.1 ± 3.3% in the striatum. In contrast, in pups receiving CPAI injection at 10 min after hypoxia ($n = 20$), the amount of tissue loss dropped to 4.7 ± 2.5% (mean ± SEM) in the cerebral cortex, 9 ± 3.2% in the hippocampus, and 9.1 ± 2.8% in the striatum ($P < 0.001$ by *t*-test) (Fig. 5*C*).

To determine the therapeutic window of CPAI treatment in this experimental model, we examined the effect of delayed CPA1 treatment after LPS/HI insult. When injected at 2 h post-hypoxia, the CPAI treatment decreased the tissue loss to 15 ± 2.6% in the cerebral cortex, 23.6 ± 4.6% in the hippocampus, and 9.1 ± 2.8% in the striatum ($n = 17$). When injected at 4 h post-hypoxia, CPAI decreased the extent of tissue loss to 15.2 ± 4% in the cerebral cortex ($P < 0.01$ compared with PBS-injection by *t*-test), 28 ± 6.1% in the hippocampus ($P < 0.05$), and 9.1 ± 2.8% in the striatum ($P = 0.07$) ($n = 18$) (Fig. 5*C*). These results suggested that a single-dose post-hypoxia injection of CPAI is sufficient to reduce infection-sensitized neonatal HI injury. Furthermore, except for the striatum (the core of infarction in this experimental model), CPAI has at least 4-h therapeutic window after LPS/HI insult for brain protection.

The CPAI Treatment of Neonatal Infection/HI Protects Near-Normal Motor Function and WM Development

Neonatal cerebral HI causes abnormal WM development and delayed neural network degeneration that correlates or contributes to motor and cognition impairment (Adams-Chapman and Stoll 2006; Stone et al. 2008; Miller and Ferriero 2009; Allin et al. 2011). Therefore, it is important to determine whether CPAI therapy protects motor function and WM development in neonatal infection/HI insult.

To this end, we conducted LPS/HI injury and PBS-versus-CPAI injection in P7 rat pups, and monitored their body weight and rotarod performance until 6 weeks of age ($n = 9$ for PBS injection, $n = 8$ for CPAI treatment, $n = 4$ for unchallenged controls). This analysis showed that PBS-injected pups initially grew slower than unchallenged animals, but reached a similar body weight after P28 (Fig. 5*D*, asterisk: $P < 0.05$ by *t*-test). Nevertheless, saline-treated animals

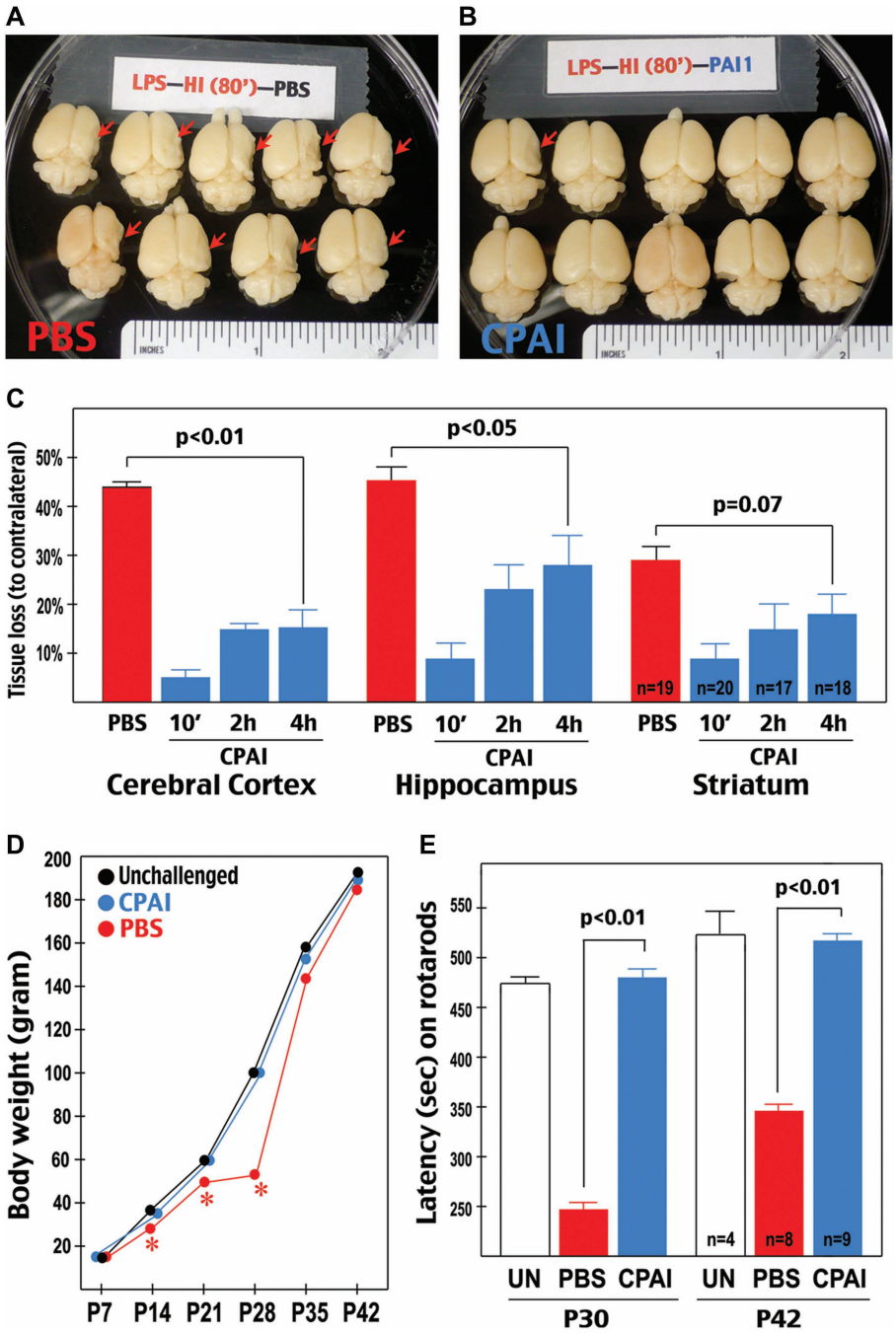

Figure 5. CPAI decreases LPS/HI-induced brain damage and impairment of motor functions. (*A* and *B*) Examples of the brains from rat pups receiving post-LPS/HI (10 min) ICV injection of saline (PBS, A) or 1.9 μg CPAI (*B*) at 7-day recovery. Note that the majority of saline-injected animals showed an obvious tissue loss on the right hemisphere (red arrows). (*C*) Quantification of tissue loss in the cerebral cortex, hippocampus, and striatum at 7 days after LPS/HI insult and ICV injection of saline (PBS) or 1.9 μg CPAI at 10 min, 2 h, or 4 h post-hypoxia. Shown are the percentages of tissue loss in each area to counterparts in contralateral hemisphere. With saline injection, there was a 43 ± 2.5% (mean ± SEM) tissue loss in the cerebral cortex, 44.2 ± 3.9% in the hippocampus, and 29.1 ± 3.3% in the striatum ($n = 19$). With CPAI injected at 10 min post-hypoxia ($n = 20$), the extent of tissue loss decreased to 4.7 ± 2.5% in the cerebral cortex, 9 ± 3.2% in the hippocampus, and 9.1 ± 2.8% in the striatum ($n = 20$). With CPAI injected at 2 h post-hypoxia, the tissue loss was 15 ± 2.6% in the cerebral cortex, 23.6 ± 4.6% in the hippocampus, and 9.1 ± 2.8% in the striatum ($n = 17$). With CPAI injection at 4 h post-hypoxia, the extent of tissue loss was 15.2 ± 4% in the cerebral cortex ($P < 0.01$ compared with saline injection by unpaired *t*-test), 28 ± 6.1% in the hippocampus ($P < 0.05$), and 9.1 ± 2.8% in the striatum ($P = 0.07$) ($n = 18$). (*D*) The body weight of unchallenged rat pups ($n = 4$) and those subjected to LPS/HI-insult at P7 followed by CPAI ($n = 8$) or saline ($n = 9$) treatment over 5-week recovery (P7–P42). Note that saline-treated rat pups initially gained body weight slower than unchallenged or CPAI-treated animals (asterisk: $P < 0.05$ by ANONA), but caught up in body weight after P28. (*E*) Comparison of the time (second) of staying on rotarods in unchallenged (UN, $n = 4$), LPS/HI-injured saline-injected (PBS, $n = 9$), and LPS/HI-injured CPAI-treated rat pups (CPAI, $n = 8$) when they reached 30 or 42 days of age. Note that the latency or falling from rotarods was significantly shorter in PBS-injected animals than that in CPAI-treated animals ($P < 0.01$ by unpaired *t*-test).

showed a significantly shorter latency on rotarods than unchallenged littermates at P30 or P42, suggesting deficits in motor coordination (Fig. 5*E*). In contrast, the LPS/HI-challenged and CPAI-treated pups manifested a growth curve and rotarod performance indistinguishable from that in unchallenged animals at P42 (Fig. 5*D* and *E*).

Next, we used ex vivo DTI to examine WM development in unchallenged ($n = 2$) and saline- or CPAI-treated rat pups ($n = 3$ for each) at 2 months of age. The rationale for using ex vivo DTI, a method that was also used in a previous study (Stone et al. 2008), is to provide a higher signal-to-noise ratio. The nerve fiber tracts were clearly visualized in directionally encoded color (DEC) maps (Fig. 6*A*). DTI parameters, including fraction anisotropy (FA), longitudinal/axial diffusivity (λ_{II}), and transverse/radial diffusivity ($\lambda_{\perp}$), were calculated in the external capsule (ec), the internal capsule (ic), and the fimbria (fm). To adjust for differences in water diffusion among fixed specimens in ex vivo DTI, we used the ratio of FA, λ_{II}, and $\lambda_{\perp}$ between the injured hemisphere (right) and the contralateral side (left) in each animal for comparison (Fig. 6*B* and *C*).

This analysis showed that neonatal LPS/HI insult caused severe truncation of external capsule and distortion of internal capsule in PBS-injected rat pups at 2 months of age (Fig. 6*A*). Hence, we focussed DTI analysis in the hippocampal fm, which retained a relatively normal trajectory in PBS-treated rats. This analysis showed that PBS-treated rats had a 30% reduction of FA and a 2-fold increase of transverse/radial diffusivity in the fm (Fig. 6*B*), a pattern consistent with demyelination of axonal tracts (Beaulieu 2002). In contrast, both CPAI-treated and unchallenged animals showed bilateral symmetry in DEC maps, and a close-to-1 R/L ratio of FA, λ_{II}, and $\lambda_{\perp}$ in ec, ic, and fm at 2 months (Fig. 6*B* and *C*).

Together, these results suggested that CPAI treatment after LPS/HI not only prevents brain atrophy, but also provides near-normal development of WM and motor functions.

Discussion

Growing evidences indicate that intrauterine infection activates fetal inflammatory response and causes greater HI brain injury in infants, but effective therapies of this condition remain unavailable for several reasons. First, infection/HI often occurs in premature neonates who are excluded from hypothermia therapy due to side effects. Secondly, systemic suppression of immune function in infants will probably increase the risk of severe infection, which already accounts for >25% of neonatal death (Lawn et al. 2005). Thirdly, intrauterine infection may alter the pathogenic responses to HI. Hence, not all therapies of pure-HI are effective in dual infection/HI insults. For example, while many therapeutics have been identified in experimental pure-HI models, to date, there is only 1 documented agent—a free radical scavenger called *N*-acetylcystein—capable of lessening LPS-sensitized HI injury (Wang et al. 2007). In this study, we examined the therapeutic potential of a stable-mutant form of PAI-1 (CPAI) that is effective against pure-HI brain injury (Yang et al. 2009). Our results revealed a critical role of nonproteolytic tPA activity in neuroinflammation and demonstrated a powerful CPAI-based therapy of infection-sensitized HI injury in neonates.

LPS Pre-Exposure Alters the Neonatal Brain Response to Hypoxia-Ischemia

In the present study, we used 4-h pretreatment with low-dose LPS (an endotoxin of Gram-negative bacteria that are a common pathogen in chorioamnionitis) and the Rice-Vannucci model of neonatal HI to challenge P7 rat pups (Eklind et al. 2005). In this model, the low-dose LPS (0.3 mg/kg) mimicked subclinical infection and caused no apparent brain injury. Yet, LPS pre-exposure markedly enhanced HI-induced BBB permeability and MMP activation in neonatal brains (Fig. 1). Previous studies have shown that LPS exposure activates innate immunity through a TLR4-MyD88-dependent pathway in neonatal brains, and either *TLR4*- or *MyD88*-null mouse pups have higher resistance to LPS-sensitized HI insults (Lehnardt et al. 2003; Wang et al. 2009). Consistent with these reports, we found that the combination of LPS pre-exposure and HI markedly increases the NF-κB signaling activity in neonatal brains, far greater than the effect by LPS- or pure-HI challenge alone (Fig. 2). Together, the present and previous studies strongly implicate the NF-κB signaling pathway as the key initiator of infection/LPS-sensitized neonatal HI injury.

An unexpected finding of our study is that dual LPS/HI insult greatly diminishes the tPA protease activity in newborn brains, while LPS exposure alone lacks this effect (Fig. 2). This pattern is intriguing, because the induction of nonvascular tPA protease activity has a pivotal role in pure-HI brain injury (Adhami et al. 2008; Yang et al. 2009). While the mechanism of LPS/HI-triggered tPA inhibition remains uncertain—1 possibility is that LPS triggers the expression of unidentified tPA-inhibitory protein at 4 h post-HI injury—our results suggests that infection/LPS pre-exposure significantly alters the response to HI in immature brains. Likewise, a previous study has shown that while *MyD88*-null mice had greater resistance to dual LPS/HI insult, they were equally sensitive to pure-HI insult like wild-type mice (Fig. 1 in Wang et al. 2009). Together, these findings suggest that pure- and infection-sensitized HI trigger divergent pathogenic responses in immature brains and may require different therapeutic strategies.

tPA Has Critical Functions for Microglia Activation in Infection-Sensitized HI Injury

Microglia, the first-line immune-response cells in the brain, have been suggested to be a convergence point for upstream infection-HI insults and downstream pathogenic mechanisms in perinatal brain injury (Khwaja and Volpe 2008; Ransohoff and Perry 2009). Once activated, microglia release cytokines and free radicals to attack neurons and oligodendrocytes (Lehnardt et al. 2003; Li et al. 2005). Moreover, many microglia-released cytokines, such as MCP-1, mediate the migration of ameboid microglial cells into the periventricular WM to induce greater neuroinflammatory response to HI, thus forming a vicious cycle of brain injury (Ivacko et al. 1997; Galasso et al. 2000). Here, we suggest that tPA has a critical role for microglia activation in neonatal HI based on our findings and those in previous studies (see below).

Briefly, it has been shown that tPA-deficient microglia had an attenuated response to LPS in cultures, and supplement of either wild-type or proteolytically inactive tPA restored the LPS response (Rogove et al. 1999). This interesting finding demonstrated that tPA has a nonproteolytic cytokine function for microglia activation. Further, by reconstituting various mutant tPA proteins, the region responsible for microglia activation was mapped to the N-terminal finger domain, distant from the C-terminal protease activity domain of tPA (Siao and Tsirka 2002). Later studies using pharmacological and genetic

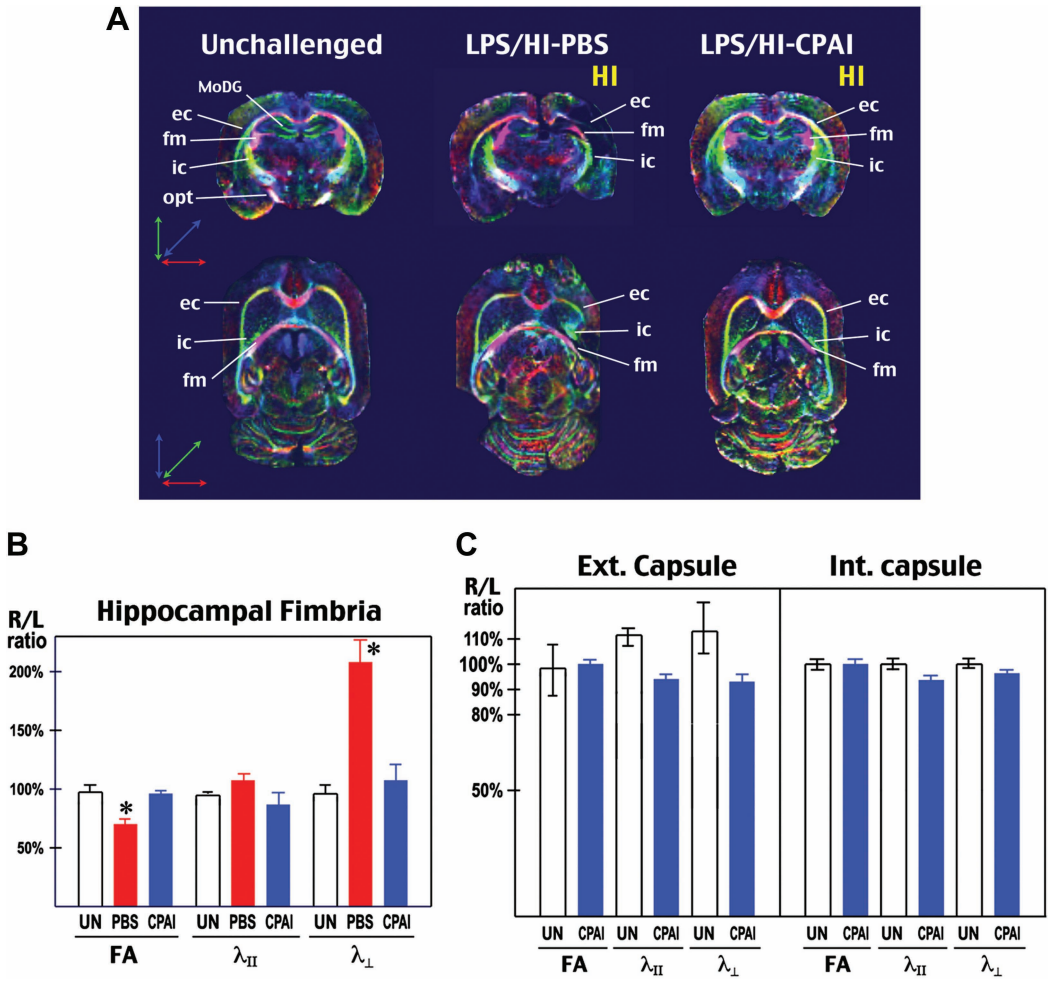

Figure 6. CPAI protects WM development of after neonatal LPS/HI injury. (*A*) Representative coronal (upper row) and transverse (lower row) images of DEC map of the brains from unchallenged (UN, $n = 2$), LPS/HI-PBS- ($n = 3$), or LPS/HI-CPAI-treated rat pups ($n = 3$) at 2 months of age. The directions of color-encoded water diffusion along *x*, *y*, and *z* axes in coronal/transverse views were indicated, respectively. Note that the DEC maps in unchallenged or LPS/HI-CPAI animals were bilaterally symmetric, while major axonal tracts in LPS/HI-PBS animals, especially ec, ic, and the fm were truncated, misplaced, or decreased in mass. MoDG, molecular layer of the dentate gyrus; opt, optic tract. (*B*) Comparison of FA, axial/longitudinal diffusivity (λ_{II}), and radial/transverse diffusivity ($\lambda_{\perp}$) in the fm by ex vivo DTI of 2-month-old animals under indicated conditions. Shown are the ratios of individual DTI parameters in the hemisphere ipsilateral to carotid-occlusion (R) and that in the contralateral hemisphere (L). The R/L ratio of FA values in LPS/HI saline-injected rats was reduced to 70 ± 6.2% (mean ± SD), while that in LPS/HI CPAI-treated animals was 96 ± 4.4%. The R/L ratio of $\lambda_{\perp}$ values was 208.6 ± 41.8% in LPS/HI saline-injected rats, compared with 108 ± 25% in CPAI-treated animals. Asterisks: $P < 0.05$ by ANOVA. (*C*) Comparison of DTI parameters in the external and internal capsule of unchallenged and LPS/HI CPAI-treated rats at 2 months of age. The R/L ratio of each DTI parameters was close to 1 in unchallenged and CPAI-treated animals.

tools suggested that tPA binds to the low-density lipoprotein receptor-related protein (LRP) on the cell surface of microglia (Zhang et al. 2007, 2009). The blockage of tPA–LRP interaction in microglia mitigates NF-κB signaling activation and reduces the infarct volume after focal ischemia in adult animals (Zhang et al. 2007, 2009).

In the present study, we demonstrated that 1) CPAI prevents LPS/HI-induced NF-κB activation (Fig. 2); 2) CPAI therapy decreases the brain MCP-1 level and the number of WM microglia/monocytes after LPS/HI insult (Fig. 3); 3) CPAI prevents microglia activation induced by direct ICV injection of LPS (Fig. 4); 4) Only tPA, but not uPA, deficiency blocks LPS-induced microglia activation (Fig. 4). Together, these results suggest that CPAI exerts protection against infection/LPS-sensitized HI injury at least in part through its inhibition of tPA-dependent microglia activation. Furthermore, the proteolytic tPA/plasmin activity can synergize with activated microglia to form a vicious cycle to further damage the immature brain (Sheehan et al. 2007; Yao and Tsirka 2011).

CPAI Mitigates Both Pure-HI and Infection-Sensitized HI Brain Injury

We recently reported that stimulation of nonvascular tPA activity plays a pivotal role for pure-HI injury in neonatal brains (Adhami et al. 2008; Yang et al. 2009). Our findings are in accord with a classical report of elevated tPA activity in fetal human brains (Gilles et al. 1971) and consistent with a large body of literature on tPA neurotoxicity (Kaur et al. 2004; Yepes et al. 2009). While a physiological-level nonvascular tPA activity may promote synaptic plasticity (Yepes et al. 2002; Samson and Medcalf 2006), excessive tPA activation in the parenchyma could elicit a multitude of harmful effects, including induction of plasmin- and MMP-mediated tissue proteolysis, escalation of glutamate excitotoxicity, microglia

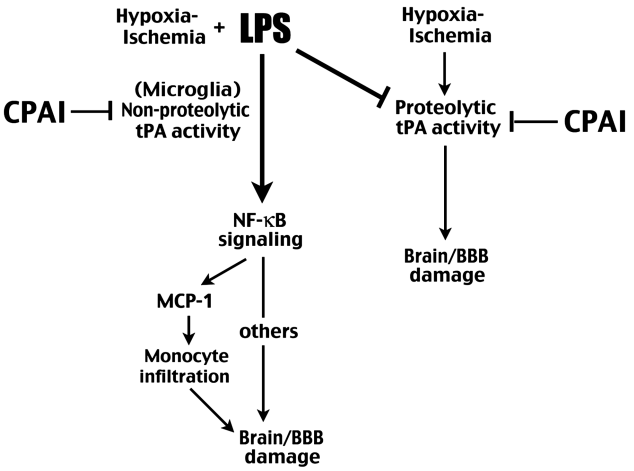

Figure 7. Summary of how infection/LPS alters the pathogenic mechanisms of HI brain injury and how CPAI provides protection in both pure-HI and infection-sensitized HI insults through inhibition of tPA activities.

activation, BBB opening, and increased monocyte diapedesis (Rogove et al. 1999; Siao and Tsirka 2002; Zhang et al. 2007, 2009; Reijerkerk et al. 2008; Su et al. 2008). Hence, anti-tPA therapy with CPAI markedly reduced pure-HI injury in neonatal brains (Berkenpas et al. 1995; Yang et al. 2009).

In the present study, we show that CPAI also strongly inhibits LPS/HI-induced NF-κB signaling and microglia activation. Thus, while LPS pre-exposure suppresses HI-induced tPA proteolytic activity in immature brains, CPAI nonetheless provides great protection (Fig. 7). Furthermore, CPAI has a long therapeutic window, being able to reduce >60% cortical atrophy by a single-dose administration at 4 h post-hypoxia. Finally, the CPAI treatment during the neonatal period confers near-normal motor and WM functions, which is an important goal in the therapy of perinatal injury to safeguard brain development (Miller and Ferriero 2009). Collectively, the remarkable properties of CPAI suggest that it is a powerful brain protection agent in neonatal HI either with or without infection. However, because intravenously injected CPAI cannot cross BBB due to its large molecular weight (~45 kDa), but may impair hemostasis in the blood, its route of drug delivery requires careful consideration. Appropriate routes include intraventricular or intranasal administration, both of which have been used to deliver large protein therapeutics in newborn brains to bypass the BBB (Whitelaw et al. 2007; Hanson and Frey 2008). Future research is warranted to examine the safety and efficacy of CPAI therapy via these routes in large-animal models of perinatal infection/HI brain injury.

In conclusion, the present study suggests a mechanism by which infection alters the response to HI in newborn brains and a powerful CPAI-based therapy of infection-sensitized HI injury in the preclinical model. These findings may provide the basis for a new therapeutic strategy of perinatal brain injury.

Funding

This work was supported by the National Institute of Health (grant NS074559 to C-Y.K) and an American Heart Association fellowship (to D.Y).

Notes

We thank Dr. Jay Degen for providing *tPA*- and *uPA*-null mice, and Drs. Ton DeGrauw and Mark Schapiro for critical reading of the manuscript. *Conflict of Interest*: None declared.

References

Adams-Chapman I, Stoll BJ. 2006. Neonatal infection and long-term neurodevelopmental outcome in the preterm infant. Curr Opin Infect Dis. 19:290–297.

Adhami F, Yu D, Yin W, Schloemer A, Burns KA, Liao G, Degen JL, Chen J, Kuan CY. 2008. Deleterious effects of plasminogen activators in neonatal cerebral hypoxia-ischemia. Am J Pathol. 172:1704–1716.

Allin MP, Kontis D, Walshe M, Wyatt J, Barker GJ, Kanaan RA, McGuire P, Rifkin L, Murray RM, Nosarti C. 2011. White matter and cognition in adults who were born preterm. PLoS One. 6: e24525.

Beaulieu C. 2002. The basis of anisotropic water diffusion in the nervous system – a technical review. NMR Biomed. 15:435–455.

Berkenpas MB, Lawrence DA, Ginsburg D. 1995. Molecular evolution of plasminogen activator inhibitor-1 functional stability. EMBO J. 14:2969–2977.

Carmeliet P, Schoonjans L, Kieckens L, Ream B, Degen J, Bronson R, De Vos R, van den Oord JJ, Collen D, Mulligan RC. 1994. Physiological consequences of loss of plasminogen activator gene function in mice. Nature. 368:419–424.

Chen GY, Nunez G. 2010. Sterile inflammation: sensing and reacting to damage. Nat Rev Immunol. 10:826–837.

Deng YY, Lu J, Ling EA, Kaur C. 2009. Monocyte chemoattractant protein-1 (MCP-1) produced via NF-kappaB signaling pathway mediates migration of amoeboid microglia in the periventricular white matter in hypoxic neonatal rats. Glia. 57:604–621.

Eklind S, Mallard C, Arvidsson P, Hagberg H. 2005. Lipopolysaccharide induces both a primary and a secondary phase of sensitization in the developing rat brain. Pediatr Res. 58:112–116.

Galasso JM, Liu Y, Szaflarski J, Warren JS, Silverstein FS. 2000. Monocyte chemoattractant protein-1 is a mediator of acute excitotoxic injury in neonatal rat brain. Neuroscience. 101:737–744.

Gilles FH, Price RA, Kevy SV, Berenberg W. 1971. Fibrinolytic activity in the ganglionic eminence of the premature human brain. Biol Neonate. 18:426–432.

Hanson LR, Frey WH, II 2008. Intranasal delivery bypasses the blood-brain barrier to target therapeutic agents to the central nervous system and treat neurodegenerative disease. BMC Neurosci. 9 (Suppl 3):S5.

Hawkins BT, Egleton RD. 2008. Pathophysiology of the blood-brain barrier: animal models and methods. Curr Top Dev Biol. 80:277–309.

Ivacko J, Szaflarski J, Malinak C, Flory C, Warren JS, Silverstein FS. 1997. Hypoxic-ischemic injury induces monocyte chemoattractant protein-1 expression in neonatal rat brain. J Cereb Blood Flow Metab. 17:759–770.

Kaur J, Zhao Z, Klein GM, Lo EH, Buchan AM. 2004. The neurotoxicity of tissue plasminogen activator? J Cereb Blood Flow Metab. 24:945–963.

Khwaja O, Volpe JJ. 2008. Pathogenesis of cerebral white matter injury of prematurity. Arch Dis Child Fetal Neonatal Ed. 93: F153–F161.

Lawn JE, Cousens S, Zupan J. 2005. 4 Million neonatal deaths: When? Where? Why? Lancet. 365:891–900.

Lehnardt S, Massillon L, Follett P, Jensen FE, Ratan R, Rosenberg PA, Volpe JJ, Vartanian T. 2003. Activation of innate immunity in the CNS triggers neurodegeneration through a Toll-like receptor 4-dependent pathway. Proc Natl Acad Sci USA. 100:8514–8519.

Lenzser G, Kis B, Snipes JA, Gaspar T, Sandor P, Komjati K, Szabo C, Busija DW. 2007. Contribution of poly(ADP-ribose) polymerase to postischemic blood-brain barrier damage in rats. J Cereb Blood Flow Metab. 27:1318–1326.

Li J, Baud O, Vartanian T, Volpe JJ, Rosenberg PA. 2005. Peroxynitrite generated by inducible nitric oxide synthase and NADPH oxidase mediates microglial toxicity to oligodendrocytes. Proc Natl Acad Sci USA. 102:9936–9941.

Lund S, Christensen KV, Hedtjarn M, Mortensen AL, Hagberg H, Falsig J, Hasseldam H, Schrattenholz A, Porzgen P, Leist M. 2006. The dynamics of the LPS triggered inflammatory response of murine microglia under different culture and in vivo conditions. J Neuroimmunol. 180:71–87.

Miller SP, Ferriero DM. 2009. From selective vulnerability to connectivity: insights from newborn brain imaging. Trends Neurosci. 32:496–505.

Nijboer CH, Heijnen CJ, Groenendaal F, May MJ, van Bel F, Kavelaars A. 2008. Strong neuroprotection by inhibition of NF-kappaB after neonatal hypoxia-ischemia involves apoptotic mechanisms but is independent of cytokines. Stroke. 39:2129–2137.

Perlman JM. 1998. White matter injury in the preterm infant: an important determination of abnormal neurodevelopment outcome. Early Hum Dev. 53:99–120.

Ransohoff RM, Perry VH. 2009. Microglial physiology: unique stimuli, specialized responses. Annu Rev Immunol. 27:119–145.

Reijerkerk A, Kooij G, van der Pol SM, Leyen T, van Het Hof B, Couraud PO, Vivien D, Dijkstra CD, de Vries HE. 2008. Tissue-type plasminogen activator is a regulator of monocyte diapedesis through the brain endothelial barrier. J Immunol. 181:3567–3574.

Rogove AD, Siao C, Keyt B, Strickland S, Tsirka SE. 1999. Activation of microglia reveals a non-proteolytic cytokine function for tissue plasminogen activator in the central nervous system. J Cell Sci. 112:4007–4016.

Samson AL, Medcalf RL. 2006. Tissue-type plasminogen activator: a multifaceted modulator of neurotransmission and synaptic plasticity. Neuron. 50:673–678.

Sheehan JJ, Zhou C, Gravanis I, Rogove AD, Wu YP, Bogenhagen DF, Tsirka SE. 2007. Proteolytic activation of monocyte chemoattractant protein-1 by plasmin underlies excitotoxic neurodegeneration in mice. J Neurosci. 27:1738–1745.

Shereen A, Nemkul N, Yang D, Adhami F, Dunn RS, Hazen ML, Nakafuku M, Ning G, Lindquist DM, Kuan CY. 2011. Ex vivo diffusion tensor imaging and neuropathological correlation in a murine model of hypoxia-ischemia-induced thrombotic stroke. J Cereb Blood Flow Metab. 31:1155–1169.

Siao CJ, Tsirka SE. 2002. Tissue plasminogen activator mediates microglial activation via its finger domain through annexin II. J Neurosci. 22:3352–3358.

Stone BS, Zhang J, Mack DW, Mori S, Martin LJ, Northington FJ. 2008. Delayed neural network degeneration after neonatal hypoxia-ischemia. Ann Neurol. 64:535–546.

Su EJ, Fredriksson L, Geyer M, Folestad E, Cale J, Andrae J, Gao Y, Pietras K, Mann K, Yepes M *et al*. 2008. Activation of PDGF-CC by tissue plasminogen activator impairs blood-brain barrier integrity during ischemic stroke. Nat Med. 14:731–737.

Tsirka SE, Rogove AD, Bugge TH, Degen JL, Strickland S. 1997. An extracellular proteolytic cascade promotes neuronal degeneration in the mouse hippocampus. J Neurosci. 17:543–552.

Volpe JJ. 2003. Cerebral white matter injury of the premature infant-more common than you think. Pediatrics. 112:176–180.

Wang X, Stridh L, Li W, Dean J, Elmgren A, Gan L, Eriksson K, Hagberg H, Mallard C. 2009. Lipopolysaccharide sensitizes neonatal hypoxic-ischemic brain injury in a MyD88-dependent manner. J Immunol. 183:7471–7477.

Wang X, Svedin P, Nie C, Lapatto R, Zhu C, Gustavsson M, Sandberg M, Karlsson JO, Romero R, Hagberg H *et al*. 2007. N-acetylcysteine reduces lipopolysaccharide-sensitized hypoxic-ischemic brain injury. Ann Neurol. 61:263–271.

Whitelaw A, Evans D, Carter M, Thoresen M, Wroblewska J, Mandera M, Swietlinski J, Simpson J, Hajivassiliou C, Hunt LP *et al*. 2007. Randomized clinical trial of prevention of hydrocephalus after intraventricular hemorrhage in preterm infants: brain-washing versus tapping fluid. Pediatrics. 119:e1071–e1078.

Yang D, Nemkul N, Shereen A, Jone A, Dunn RS, Lawrence DA, Lindquist D, Kuan CY. 2009. Therapeutic administration of plasminogen activator inhibitor-1 prevents hypoxic-ischemic brain injury in newborns. J Neurosci. 29:8669–8674.

Yao Y, Tsirka SE. 2011. Mouse MCP1 C-terminus inhibits human MCP1-induced chemotaxis and BBB compromise. J Neurochem. 118:215–223.

Yepes M, Roussel BD, Ali C, Vivien D. 2009. Tissue-type plasminogen activator in the ischemic brain: more than a thrombolytic. Trends Neurosci. 32:48–55.

Yepes M, Sandkvist M, Coleman TA, Moore E, Wu JY, Mitola D, Bugge TH, Lawrence DA. 2002. Regulation of seizure spreading by neuroserpin and tissue-type plasminogen activator is plasminogen-independent. J Clin Invest. 109:1571–1578.

Yin W, Signore AP, Iwai M, Cao G, Gao Y, Johnnides MJ, Hickey RW, Chen J. 2007. Preconditioning suppresses inflammation in neonatal hypoxic ischemia via Akt activation. Stroke. 38:1017–1024.

Zhang C, An J, Strickland DK, Yepes M. 2009. The low-density lipoprotein receptor-related protein 1 mediates tissue-type plasminogen activator-induced microglial activation in the ischemic brain. Am J Pathol. 174:586–594.

Zhang X, Polavarapu R, She H, Mao Z, Yepes M. 2007. Tissue-type plasminogen activator and the low-density lipoprotein receptor-related protein mediate cerebral ischemia-induced nuclear factor-kappaB pathway activation. Am J Pathol. 171:1281–1290.